Ice-dammed lake drainage in west Greenland: Drainage pattern and implications on ice flow and bedrock motion

Kjeldsen, Kristian Kjellerup; Khan, Shfaqat Abbas; Bjørk, Anders; Nielsen, Karina; Mouginot, Jeremie

Published in:
Geophysical Research Letters

Link to article, DOI:
10.1002/2017GL074081

Publication date:
2017

Document Version
Publisher's PDF, also known as Version of record

AGU PUBLICATIONS

Geophysical Research Letters

RESEARCH LETTER
10.1002/2017GL074081

Key Points:
- The period between drainage events has shortened from 10 to 5 years, coinciding with thinning of the damming glacier since the late 1990s
- Within 7 days, 1.83 ± 0.17 km^3 of water was released subglacially to a nearby fjord, leading to speedup of the damming glacier
- Rapid drainage caused 18.6 ± 0.1 mm of instantaneous elastic bedrock uplift in agreement with GPS data recorded adjacent to the lake

Correspondence to:
K. K. Kjeldsen,
kkjeldsen@snm.ku.dk

Citation:
Kjeldsen, K. K., S. A. Khan, A. A. Bjørk, K. Nielsen, and J. Mouginot (2017), Ice-dammed lake drainage in west Greenland: Drainage pattern and implications on ice flow and bedrock motion, *Geophys. Res. Lett.*, *44*, 7320–7327, doi:10.1002/2017GL074081.

Received 8 MAY 2017
Accepted 1 JUL 2017
Accepted article online 6 JUL 2017
Published online 18 JUL 2017

Ice-dammed lake drainage in west Greenland: Drainage pattern and implications on ice flow and bedrock motion

Kristian K. Kjeldsen[1,2,3], Shfaqat A. Khan[3], Anders A. Bjørk[2,4,5], Karina Nielsen[3], and Jeremie Mouginot[4]

[1]Department of Earth Sciences, University of Ottawa, Ottawa, Ontario, Canada, [2]Centre for GeoGenetics, Natural History Museum of Denmark, University of Copenhagen, Copenhagen, Denmark, [3]Department of Geodesy, DTU Space, National Space Institute, Technical University of Denmark, Kongens Lyngby, Denmark, [4]Department of Earth System Science, University of California, Irvine, California, USA, [5]NASA Jet Propulsion Laboratory, Pasadena, California, USA

Abstract Ice-dammed lakes drain frequently in Greenland, but the impacts of these events differ between sites. Here we study the quasi-cyclic behavior of the ~40 km^2 Lake Tininnilik in west Greenland and its impact on ice flow and crustal deformation. Data reveal rapid drainage of 1.83 ± 0.17 km^3 of water in less than 7 days in 2010, leading to a speedup of the damming glacier, and an instantaneous modeled elastic bedrock uplift of 18.6 ± 0.1 mm confirmed by an independent lakeside GPS record. Since ice-dammed lakes are common on Greenland, our results highlight the importance of including other sources of surface loading in addition to ice mass change, when assessing glacial isostatic adjustment or elastic rebound using geodetic data. Moreover, the results illustrates a linkage between subglacial discharge and ice surface velocity, important for assessing ice flux, and thus mass balance, in a future warming climate.

1. Introduction

Ice-dammed lakes are abundant along the entire periphery of the Greenland Ice Sheet and by storing water they act as a buffer between the ice sheet runoff and the surrounding ocean. The drainage rate varies considerably, ranging from gradual discharge to sudden catastrophic flood events, independent of the terminal regime of the damming glacier [*Russell*, 1989; *Russell et al.*, 2011; *Weidick and Citterio*, 2011; *Kjeldsen et al.*, 2014]. These events can have implications on the fjord circulation because they push large volumes of buoyant, subglacial freshwater to the ocean surface [*Kjeldsen et al.*, 2014]. They can also rework the morphology of proglacial outwash plains [*Russell et al.*, 2011] and can cause bedrock displacements, detectable from remote sensing data [*Furuya and Wahr*, 2005].

In this study we examined the changes during the period from 1997 to 2016 of Lake Tininnilik, an ~ 40 km^2 ice-dammed lake in central west Greenland (Figure 1a). The lake is located about 50 km from Jakobshavn Isbræ and is dammed by the Sarqardliup Sermia outlet glacier, which has remained largely stable during the past 150 years [*Weidick*, 1994], with limited mass loss during the twentieth century [*Kjeldsen et al.*, 2015]. Fifteen historic observations reveal that during 1942–1983, Lake Tininnilik drained approximately once every tenth year [*Braithwaite and Thomsen*, 1984]. This trend continued until 2003, with drainage events in 1993 and 2003 causing estimated water level changes of ~75 m and a volume reduction of ~2.3 km^3 [*Furuya and Wahr*, 2005].

We assessed water level changes during the study period, using airborne and spaceborne altimetry data, digital elevation models (DEMs), and optical satellite data. Aerial photographs were used to generate a high-resolution DEM, from which we computed lake volume changes. We also assessed surface changes of the damming ice over the same period, examined the impact on ice flow, and estimated the elastic deformation of the crust. These estimates were consistent with changes in vertical land motion measured independently from a lakeside GPS station.

2. Data and Methods

2.1. Aerial Photographs and DEM

In August 2011 we collected 235 oblique aerial photographs from a helicopter flying at an altitude of 1–1.5 km (Figure 1). From these, we created a 0.5 m orthophoto and a 2 m high-resolution DEM

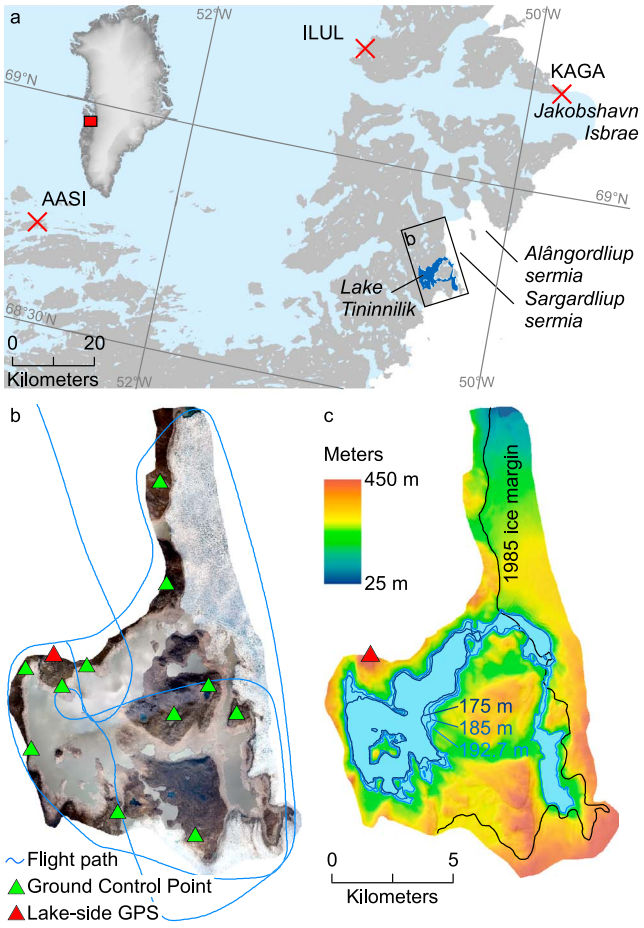

Figure 1. (a) Overview map of Lake Tininnilik and the surrounding area, including the location of the GNET-GPS-receiver in red crosses, (b) orthophoto and digital elevation model (c) of the lake based on 235 oblique photos and 11 ground-control points. Also illustrated in Figure 1c is the lake extent digitized from optical satellite imagery close in time to altimetry observations, the 1985 ice margin, and the location of a lakeside GPS receiver.

(Figures 1b and 1c) using Agisoft version 1.1. In order to coregister the DEM to the WGS84 ellipsoid, we used 11 ground control points and measured the coordinates in aerotriangulated vertical stereo photogrammetric imagery [*Korsgaard et al.*, 2016]. Lake extent was digitized on the derived orthophoto, and the water level (192.7 m) was obtained by continuing the interpolation between two altimetry recordings obtained 3 weeks earlier. To improve the bathymetry, lake extent was digitized on optical satellite imagery during low water levels in 2010 and 2015, as close in time as possible to altimetry recordings. We assessed the uncertainty of the DEM using all available data from NASA's Airborne Topographic Mapper (ATM) on solid bedrock and excluded data on slopes greater than 20° to account for the impact of slope-induced error [*Korsgaard et al.*, 2016]. After filtering for slope the DEM has a mean bias of 0.5 m and standard deviation of 4.1 m, based on 1637 data points distributed across the DEM.

2.2. Remote Sensing Data, Elevation Changes, and Ice Flow

To assess lake water level and ice surface changes between 1997 and 2016, we used ICESat GLA12 Release 34 data [*Zwally et al.*, 2011], with a crossover standard deviation of 0.2 m [*Howat et al.*, 2008; *Pritchard et al.*, 2009] and NASA's ATM and Land, Vegetation and Ice Sensor (LVIS) flight lines [*Blair and Hofton*, 2013; *Krabill*, 2014], both of which have an uncertainty of 0.1 m. Moreover, we obtained lake level elevations from CryoSat-2, based on the ESA baseline C level 1b product, using the methodology outlined by *Jiang et al.* [2017]. Observations were also extracted from AeroDEM (August 1985) [*Korsgaard et al.*, 2016] and ArcticDEM (April 2013 and August 2015; http://pgc.umn.edu/arcticdem) [*Noh and Howat*, 2015], and we used Landsat, Sentinel-2, Advanced Spaceborne Thermal Emission and Reflection (ASTER), and Moderate Resolution Imaging Spectroradiometer (MODIS) archive satellite imagery (http://earthexplorer.usgs.gov), to provide a qualitative assessment of lake changes, for instance, to determine whether the lake had drained or not.

For the water level time series, we combined all data that intersect the lake at a given time stamp and discard obvious outliers as these reflect smaller icebergs. We used the standard deviation or the reported uncertainty, depending on which was larger, as a measure of uncertainty of the water level. Over ice we defined locations where the ATM, LVIS, and ICESat tracks overlap. Within a 100 m radius around these locations, we extracted the evolution of the mean elevation (including DEMs) and used the standard deviation as uncertainty.

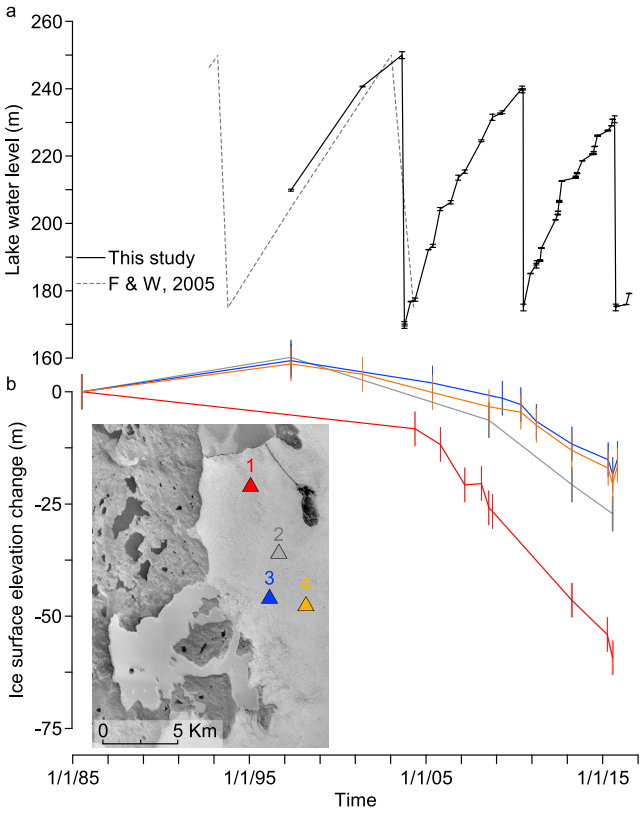

Figure 2. (a) Water level changes of Lake Tininnilik based on different sensors and lake level changes from *Furuya and Wahr* [2005]. The record shows that the time between events was decreasing from every approximately tenth year to ~5 years between the last two events and, moreover, that the lake level prior to the drainage events has been decreasing during the past events. These multidecadal changes coincided with net thinning of the damming glacier. (b) Ice surface elevation change relative to the 1985 ice surface elevation. Since then the glacier has experienced a net thinning, though at higher locations (Loc. 2–Loc. 4) there was a slight thickening between 1985 and 1997.

To examine the impact of lake drainage on ice flow, ice velocity time series between January 2014 and December 2016 were constructed using Sentinel-1/ESA, Landsat-8/USGS, and RADARSAT-2/CSA [*Mouginot et al.*, 2017]. Uncertainties on the ice velocity estimates range from 10 m/yr to 50 m/yr depending on the sensors used and time interval between acquisitions.

2.3. Observed and Modeled Elastic Rebound

We examined vertical land motion from a lakeside GPS station (Figure 1) that recorded data during 190 and 109 days in 2010 and 2012, respectively. The GPS data were processed using the GIPSY OASIS v6.4 software package following the procedure outlined by *Khan et al.* [2010]. The elastic rebound was modeled using the standard setup of the Regional ElAstic Rebound (REAR) calculator [*Melini et al.*, 2015]. In order to compute surface rates of displacements in response to a disc load of uniform thickness (Green Functions for vertical displacements), REAR uses load deformation coefficients, based on the seismological Earth model STW105 [*Kustowski et al.*, 2008]. Next changes in surface loading, i.e., changes in water level, are superimposed to model the elastic rebound. We used a disc-shaped load function with a radius of approximately 11 m, equivalent to 400 m^2. The uncertainty of the modeled rebound was estimated by computing the elastic uplift due to a uniform 20 cm (equal to the combined uncertainty of two altimetry recordings) load change over the largest lake extent.

3. Results and Discussion

3.1. Water Level Changes

Figure 2a shows the water level changes between 13 May 1997 and 3 July 2016 based on a compilation of airborne and satellite altimetric data. Satellite imagery proved important as drainage events in 2003 and 2010 were bracketed in time by these observations. Visual inspection of the imagery was used to determine whether the lake was full at a given point in time between altimetry observations. Importantly, we found that the maximum water level prior to drainage in 2003 was ~250 m based on comparing lake extent on satellite imagery to the DEM. In 2010 lake level prior to drainage was 239.8 m, while before the 2015 event minimum water level was 230.9 m (Figure 2a). For the 2010 and 2015 events comparison between lake extent and the DEM suggested a postevent water level lower than ~175 m, leading to a lowering of >65 m. Around the lake, several shorelines mark previous high water levels with the most pronounced being found at 260 m at the boundary between the continuous vegetation cover above and highest previous water level, which

suggest a previous, more extensive ice damming, perhaps during the Little Ice Age. The detailed time series of water level changes shows that the time interval between drainage events has decreased from 10 years prior to 2003, to 6.8 years between the 2003 and 2010 events to 5.1 years between the 2010 and 2015 events.

To estimate lake volume change during drainage events, we used the high-resolution DEM (Figure 1c). The aerial imagery was acquired in August 2011, a little more than a year after the previous drainage event, when the water level was rising. To improve the DEM, lower levels were added by combining satellite-derived lake extent and altimetry observation following drainage events. For the three events the water volume drained from the lake ranged between 1.48 ± 0.16 and 2.28 ± 0.17 km^3. These estimates agreed well with previous studies, for instance using historical imagery and maps (1.69 km^3) [*Braithwaite and Thomsen*, 1984] and satellite interferometry, a simplified outline of the lake, and a coarser DEM (2.3 km^3) [*Furuya and Wahr*, 2005].

For all three recent drainage events, and the 1993 event, water exited the lake in the northeastern corner and flowed beneath the damming glacier. Assessment of the exact timing of the three events was limited by cloud conditions and the available imagery, in particular, for the 2003 event; thus, we focused on the 2010 and 2015 events. Combining the altimetry, GPS, and satellite observations showed that the maximum duration of the 2003 drainage event was 48 days, the 2010 event 25 days, and that of the 2015 event 20 days. The availability of a suite of different satellite data showed that the duration estimates found here were several orders of magnitude shorter than what was proposed by *Braithwaite and Thomsen* [1984], who estimated 1.0–1.5 years of drainage before the lake started to refill during 1942–1983.

A better control on the rate of lake drainage was available for the 2010 event, when GPS data showed that drainage started on 30 June/1 July (Figure 4). Combining the DEM and Landsat imagery showed considerable drainage on 7 July, when the lake extent was roughly equivalent to that of the 175–177 m elevation level. After this, the lake continued to drain until at least the 16 July, though by the 25 July changes were less certain; however, already on 10 August, the lake was starting to fill again. This meant that though the duration of the 2010 event was 25 days, 1.83 ± 0.17 km^3 of water was emptied within only 7 days.

3.2. Ice Surface Changes Since 1985

The lake is dammed by Sargardliup Sermia outlet glacier (Figure 1). The change of ice surface elevation at four locations was assessed relative to the 1985 ice surface (Figure 2b). The lowermost location (Loc. 1) showed net thinning during the entire timespan, with increased rates from March 2007 onward, resulting in a net surface lowering of ~60 m. It should be noted that no data exist between August 1985 and May 2004. The three locations at higher elevation showed net thinning, although less pronounced relative to Loc. 1, but interestingly, also an ~ 7 m thickening of the glacier by May 1997. This was followed by a thinning that caused a continually steepening of the ice surface profile toward the calving front and away from the lake. For Loc. 2 the net thinning was ~27 m, while that of Loc. 3 and Loc. 4 was ~15 m and ~16 m, respectively.

The changes in ice surface elevation coincided with changes in water level height prior to drainage and changes in the volume capacity of the lake (Figure 2). Estimates of the changes related to the 1993 drainage event were of similar magnitude to the 2003 event [*Furuya and Wahr*, 2005], suggesting a stable maximum lake storage capacity between at least 1993 and 2003. Continuous and increased thinning after 1997 and 2010, respectively, coupled with continually lower and decreasing lake levels prior to drainage, combined to produce continuously smaller drained volumes. This pattern underscores the direct relation between the thickness of the damming glacier and the maximum water storage capacity of the ice-dammed lake (Figure 2).

3.3. Glacial Speedup and Subglacial Drainage Path

Using high-resolution time series of ice velocity (Figure 3), extracted from two streams within Sarqardliup Sermia, we assessed the impact of lake drainage on the damming ice and inferred the subglacial drainage path. Both series clearly showed a seasonal pattern with velocities increasing from May, reaching peak values in June that were about 2 times higher than the general annual level. Similar seasonal patterns have been found elsewhere using GPS [e.g., *Ahlstrøm et al.*, 2013], and remote sensing [e.g., *Moon et al.*, 2014; *Mouginot et al.*, 2017]. Interestingly, at Loc. 5 (Figure 3a) velocities increase considerably in September 2015, which coincided with the lake drainage event. On the contrary, the velocity remained largely unchanged at Loc. 6 during the same time (Figure 3b). Following this drainage-induced speedup at Loc. 5,

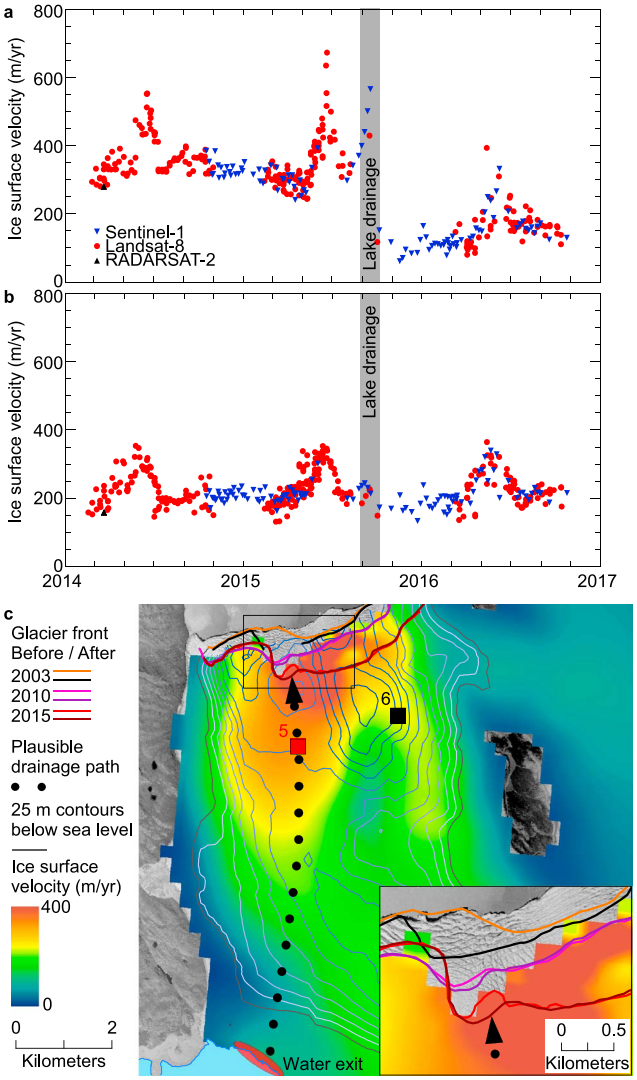

Figure 3. Velocity time series from (a) Loc. 5 and (b) Loc. 6. Both locations show a clear seasonal cycle; however, in September 2015 Loc. 5 experienced a speedup that coincided with the 2015 drainage event. (c) The difference in ice velocity between Loc. 5 and Loc. 6, the localized retreat of the glacier terminus (insert), and that water drained from the lake through the northeastern corner (red oval circle) led to a plausible drainage path.

velocities decreased to a level lower than before the event. This was caused by changes in the subglacial hydrologic network, likely due to enlarged subglacial channels, which would more effectively drain the subglacial discharge, leading to a decrease in basal pressure, and, ultimately, a slowdown of the ice due to higher drag over the bed, as described elsewhere along the western part of the ice sheet [e.g., *van de Wal et al.*, 2008; *Sole et al.*, 2011].

Moreover, visible imagery of the glacier terminus before and after drainage events in 2003, 2010, and 2015, illustrated that the calving front was generally stable except along a specific stretch of the terminus, where localized retreat was observed following each of the three events (insert on Figure 3c). This stretch was located downstream of Loc. 5 where a speedup was detected.

The fact that water exited the lake at the northeast corner (red oval circle on Figure 3c), coupled with the speedup recorded at Loc. 5 and the retreat of the calving front following drainage, suggested that the lake drained through a specific part of the subglacial drainage network (Figure 3c).

3.4. Observed and Modeled Rapid Elastic Rebound

To assess the impact of lake drainage on bedrock motion, we exploited data from a GPS receiver located adjacent to Lake Tininnilik (Figure 4), and using the derived lake volume change, we estimated the corresponding elastic response of the Earth's crust. The GPS recorded the response of the crust to elastic and viscoelastic displacement (GIA) from present-day mass changes and from past ice changes since the last glacial maximum, respectively.

Figure 4b shows the GPS signal after the elastic uplift and GIA were removed, based on ice mass changes during April 2009 to April 2012 [*Khan et al.*, 2014] and the average GIA at the GNET-GPS stations [*Khan et al.*, 2016], which combined yielded 15.2 ± 2.4 mm/yr. This produced a time series where changes due to fluctuations in lake level (Figure 4a) were more directly apparent.

During 2010 the GPS recorded a considerable, short-lived uplift of 23.7 ± 7.0 mm within 3 days, followed by a continual uplift, albeit at a decreasing rate. This excursion from the general pattern coincided with the 2010 drainage event. Part of uplift may be due to a day-to-day variability, which prior to the event was up to 7 mm, leading to a standard deviation of 2.6 mm; thus, relative to the average level obtained during the preevent

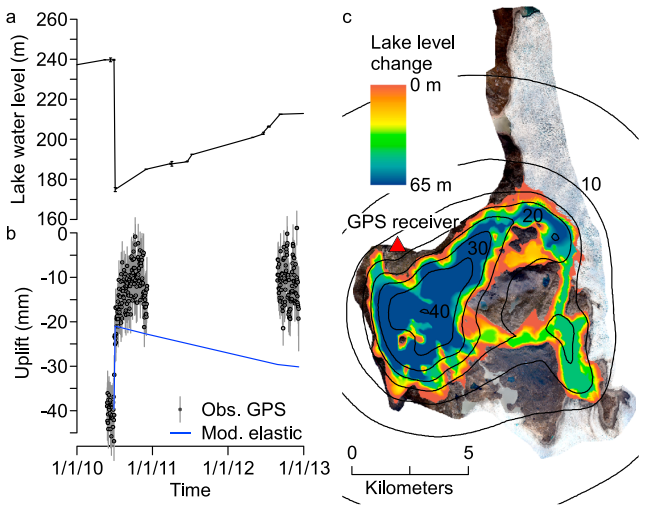

Figure 4. (a) Water level changes during 2010–2012. (b) GPS record and the associated uncertainty from the lakeside receiver, corrected for elastic rebound due to ice sheet mass loss and GIA, and the modeled elastic response due to changes in lake volume. In response to the 2010 drainage event, the estimated elastic bedrock uplift is 18.6 ± 0.1 mm, which agreed well with the recorded 17.1 ± 6.9 mm uplift in 3 days. (c) Change in surface loading related to drainage events generated a distinct spatial pattern of the elastic response that illustrated localized changes.

period, this yielded an uplift of 17.1 ± 6.9 mm in 3 days. Following the drainage event the daily and seasonal variability [*Bevis et al.*, 2012] again begins to be more pronounced in the signal, a trend that was also evident in the 2012 record.

Figure 4b shows the modeled elastic response due to lake changes during mid-2010 to late 2012. In 2010 water level dropped from 239.8 m to ~175 m, resulting in a volume change of 1.83 ± 0.17 km^3 within 7 days, possibly even slightly more due to continual drainage. Using REAR, this led to a modeled elastic uplift of 18.6 ± 0.1 mm. As drainage continued for an additional 18 days, bedrock uplift would have continued in response to water exiting the lake, although 25 days after the event water was beginning to fill the lake again. The elastic response was very localized, yielding a distinct spatial pattern, with changes of >40 mm occurring in the center of the lake basin, while ~5–7 km from the lake edge the elastic response was 5 mm (Figure 4c). Following the drainage event the net effect of water filling from 175 m to 185.1 m on December 2 2010, which almost covered the 2010 GPS time series, was a modeled elastic response of −1.8 ± 0.1 mm.

During the gap period the lake fills from 185.1 m to 211.1 m, interpolated between observations, causing an modeled elastic uplift of −6.8 ± 0.1 mm, while overlapping the 2012 GPS time series water level changed from 211.1 m to 212.9 m, yielding a modeled elastic uplift of −0.6 ± 0.1 mm.

Unraveling the bedrock motion due to continual drainage following the event in 2010 and the negative uplift in response to lake filling proved difficult as the response to daily and seasonal atmospheric and ice mass variability outweighs the signal from the lake. The difference between the elastic motion due to lake filling, causing negative uplift, and the GPS time series, corrected for average April 2009 to April 2012 ice mass loss and GIA, suggested that during 2012 there was an additional change in surface loading in the vicinity of the lake. A possible explanation was the speedup and increased discharge of Jakobshavn Isbrae in 2012 relative to previous years [*Enderlin et al.*, 2014; *Muresan et al.*, 2016]; however, a long time series after 2012 is needed from the GPS receiver to properly assess the impact of such changes.

4. Conclusions

Drainage of ice-dammed lakes occur frequently in Greenland; however, the manner in which they drain varies greatly leading to considerably different impact on their surroundings. Here we assessed the changes of Lake Tininnilik using different remote sensing platforms and found that following a more stable behavior since 1942 with drainages occurring approximately every tenth year, the last two events were ~5 years apart with a 44% decrease in storage capacity from 2.28 ± 0.17 km^3 to 1.48 ± 0.16 km^3 between at least 2003 and 2015. These changes coincided with a 6–7 m thickening of the damming glacier between 1985 and 1997, followed by thinning of the damming glacier since 1997, leading to ~60 m net surface lowering near the glacier front and ~15–16 m net surface lowering closer to the ice-dammed lake.

Moreover, ice velocity clearly showed a localized speedup in relation to the 2015 event, followed by lower velocities afterward. Combining the spatial velocity pattern and glacier terminus positions suggested that the subglacial path, through which the water drained from the lake, was very localized.

The change in surface loading during the 2010 drainage event led to a predicted 18.6 ± 0.1 mm instantaneous elastic bedrock uplift at the lakeside GPS site, with a distinct spatial pattern due to the spatial characteristics of the lake. This estimate was in good agreement with a time series from the lakeside GPS receiver that recorded a 17.1 ± 6.9 mm uplift in 3 days, relative to the average vertical preevent position.

These results have multiple implications: first, assessing changes in the areal extent of ice-dammed lakes during past century will allow long-term perspectives on the interaction between the damming ice and climate. Second, the observed and modeled elastic rebound presented here underlines the importance of considering additional sources of surface loading in addition to ice mass change, when assessing GIA and elastic rebound from geodetic data, important not only in Greenland but also elsewhere. Third, ice velocity measurements reveal a characteristic annual cycle that locally becomes modulated due to large-scale injection of water to the base of the glacier, causing a considerable speedup, and in this case, a subsequent decrease in velocity, important for assessing ice flux, and thus mass balance, in a future warming climate.

Acknowledgments
K.K.K. and A.A.B. were supported by the Danish Council Research for Independent research grants DFF-4090-00151 and DFF-610800469, respectively, and A.A.B. was further supported by the Inge Lehmann Scholarship from the Royal Danish Academy of Science and Letters. The authors would like to thank Jeff Freymueller and Matt King for valuable comments and constructive feedback. Results produced in this study are available through the corresponding author.

References

Ahlstrøm, A. P., et al. (2013), Seasonal velocities of eight major marine-terminating outlet glaciers of the Greenland ice sheet from continuous in situ GPS instruments, *Earth Syst. Sci. Data*, *5*(2), 277–287, doi:10.5194/essd-5-277-2013.

Bevis, M., et al. (2012), Bedrock displacements in Greenland manifest ice mass variations, climate cycles and climate change, *Proc. Natl. Acad. Sci. U.S.A.*, doi:10.1073/pnas.1204664109.

Blair, B., and M. Hofton (2013), *IceBridge LVIS L2 Geolocated Ground Elevation and Return Energy Quartiles, [2010–2013]*, Natl. Snow and Ice Data Cent., Boulder, Colo.

Braithwaite, R. J., and H. H. Thomsen (1984), Runoff conditions at Kuussuup Tasia, Christianshåb, estimated by modelling, *Grønlands Geol. Undersøgelser, Gletscher-hydrologiske Meddelser*, *2*, 1–23.

Enderlin, E. M., I. M. Howat, S. Jeong, M.-J. Noh, J. H. van Angelen, and M. R. van den Broeke (2014), An improved mass budget for the Greenland ice sheet, *Geophys. Res. Lett.*, *41*, 866–872, doi:10.1002/2013GL059010.

Furuya, M., and J. M. Wahr (2005), Water level changes at an ice-dammed lake in west Greenland inferred from InSAR data, *Geophys. Res. Lett.*, *32*, L14501, doi:10.1029/2005GL023458.

Howat, I. M., B. E. Smith, I. R. Joughin, and T. A. Scambos (2008), Rates of southeast Greenland ice volume loss from combined ICESat and ASTER observations, *Geophys. Res. Lett.*, *35*, L17505, doi:10.1029/2008GL034496.

Jiang, L., K. Nielsen, O. B. Andersen, and P. Bauer-Gottwein (2017), Monitoring recent lake level variations on the Tibetan Plateau using CryoSat-2 SARIn mode data, *J. Hydrol.*, *544*, 109–124, doi:10.1016/j.jhydrol.2016.11.024.

Khan, S. A., L. Liu, J. Wahr, I. M. Howat, I. R. Joughin, T. van Dam, and K. Fleming (2010), GPS measurements of crustal uplift near Jakobshavn Isbræ due to glacial ice mass loss, *J. Geophys. Res.*, *115*, B09405, doi:10.1029/2010JB007490.

Khan, S. A., et al. (2014), Sustained mass loss of the northeast Greenland ice sheet triggered by regional warming, *Nat. Clim. Change*, *4*, 292–299, doi:10.1038/nclimate2161.

Khan, S. A., et al. (2016), Geodetic measurements reveal similarities between post–Last glacial maximum and present-day mass loss from the Greenland ice sheet, *Sci. Adv.*, *3*(9), doi:10.1126/sciadv.1600931.

Kjeldsen, K. K., J. Mortensen, J. Bendtsen, D. Petersen, K. Lennert, and S. Rysgaard (2014), Ice-dammed lake drainage cools and raises surface salinities in a tidewater outlet glacier fjord, west Greenland, *J. Geophys. Res. Earth Surf.*, *119*, 1310–1321, doi:10.1002/2013JF003034.

Kjeldsen, K. K., et al. (2015), Spatial and temporal distribution of mass loss from the Greenland Ice Sheet since AD 1900, *Nature*, *528*(7582), 396–400, doi:10.1038/nature16183.

Korsgaard, N. J., C. Nuth, S. A. Khan, K. K. Kjeldsen, A. A. Bjørk, A. Schomacker, and K. H. Kjær (2016), Digital elevation model and orthophotographs of Greenland based on aerial photographs from 1978–1987, *Sci. Data*, *3*, 160032, doi:10.1038/sdata.2016.32.

Krabill, W. B. (2014), *IceBridge ATM L2 Icessn Elevation, Slope, and Roughness, [1997–2015]*, Natl. Snow and Ice Data Cent., Boulder, Colo.

Kustowski, B., G. Ekström, and A. M. Dziewomski (2008), Anisotropic shear-wave velocity structure of the Earth's mantle: A global model, *J. Geophys. Res.*, *113*, B06306, doi:10.1029/2007JB005169.

Melini, D., P. Gegout, M. King, B. Marzeion, and G. Spada (2015), On the rebound: Modeling Earth's ever-changing shape, *Eos*, *96*, 1–2, doi:10.1029/2015EO033387.

Moon, T., I. Joughin, B. Smith, M. R. Broeke, W. J. Berg, B. Noël, and M. Usher (2014), Distinct patterns of seasonal Greenland glacier velocity, *Geophys. Res. Lett.*, *41*, 7209–7216, doi:10.1002/2014GL061836.

Mouginot, J., E. Rignot, B. Scheuchl, and R. Millan (2017), Comprehensive annual ice sheet velocity mapping using Landsat-8, Sentinel-1, and RADARSAT-2 data, *Remote Sens.*, *9*(4), doi:10.3390/rs9040364.

Muresan, I. S., S. A. Khan, A. Aschwanden, C. Khroulev, T. van Dam, J. Bamber, M. R. Van Den Broeke, B. Wouters, P. K. Munneke, and K. H. Kjær (2016), Modelled glacier dynamics over the last quarter of a century at Jakobshavn Isbræ, *Cryosphere*, *10*, 597–611, doi:10.5194/tc-10-597-2016.

Noh, M., and I. M. Howat (2015), Automated stereo-photogrammetric DEM generation at high latitudes: Surface Extraction with TIN-based Search-space Minimization (SETSM) validation and demonstration over glaciated regions, *GIScience Remote Sens.*, *52*(2), 198–217, doi:10.1080/15481603.2015.1008621.

Pritchard, H. D., R. J. Arthern, D. G. Vaughan, and L. A. Edwards (2009), Extensive dynamic thinning on the margins of the Greenland and Antarctic ice sheets, *Nature*, *461*(7266), 971–5, doi:10.1038/nature08471.

Russell, A. J. (1989), A comparison of two recent jökulhlaups from an ice-dammed lake, Søndre Strømfjord, West Greenland, *J. Glaciol.*, *35*(120), 157–162.

Russell, A. J., J. L. Carrivick, T. Ingeman-nielsen, J. C. Yde, and M. Williams (2011), A new cycle of jökulhlaups at Russell Glacier, Kangerlussuaq, West Greenland, *J. Glaciol.*, *57*(202), 238–246.

Sole, A. J., D. W. F. Mair, P. W. Nienow, I. D. Bartholomew, M. A. King, M. J. Burke, and I. R. Joughin (2011), Seasonal speedup of a Greenland marine-terminating outlet glacier forced by surface melt–induced changes in subglacial hydrology, *J. Geophys. Res.*, *116*, F03014, doi:10.1029/2010JF001948.

van de Wal, R. S. W., W. Boot, M. R. van den Broeke, C. J. P. P. Smeets, C. H. Reijmer, J. J. A. Donker, and J. Oerlemans (2008), Large and rapid melt-induced velocity changes in the Ablation Zone of the Greenland ice sheet, *Science*, *321*(111), 2008–2011, doi:10.1126/science.1158540.

Weidick, A. (1994), Historical fluctuations of calving glaciers in South and West Greenland, *Rapp. Geol. Surv. Greenl.*, *161*, 73–79.

Weidick, A., and M. Citterio (2011), The ice-dammed lake Isvand, West Greenland, has lost its water, *J. Glaciol.*, *57*(201), 186–188.

Zwally, H. J., R. Schutz, J. Bentley, T. Herring, J. Minster, J. Spinhirne, and R. Thomas (2011), *GLAS/ICESat L2 Antarctic and Greenland Ice Sheet Altimetry Data V031*, Natl. Snow and Ice Data Cent., Boulder, Colo.